A Solitary Wave-Based Tonometer for Intraocular Pressure Measurement

PIERVINCENZO RIZZO[1], MADISON HODGSON[2], ALI KOMAIE[3] and SAMUEL J. DICKERSON[4]

ABSTRACT

Glaucoma is an age-related incurable disease and the second cause of blindness in the world. The risk of developing glaucoma increases in the presence of elevated intraocular pressure (IOP), a risk factor that can be modified through invasive surgery. In clinical practice, IOP remains the cornerstone of the diagnosis and management of glaucoma, and Goldmann applanation tonometry (GAT) is considered the gold standard in IOP measurements. However, GAT, as any other commercial system, provides a single data point value that is unable to frame the natural circadian rhythm and sporadic surges of IOP. This capability is only possible with a portable device that patients can eventually self-administer anytime anywhere. To serve the purpose, the device must be easy-to-use and not requiring sterilization or topical anesthesia. Additional desirable features are low price and adaptability to patient's eyeball geometry. To address these needs, our group has conceptualized, assembled, and tested a new tonometer based on highly nonlinear solitary waves propagating along a chain of particles, the last of which is in dry contact with the eye to be evaluated. The hypothesis is that the time of flight (ToF) of the waves within the chain is monotonically associated with the IOP. In this study, the effect of central corneal thickness (CCT) and IOP of artificial corneas made of polydimethylsiloxane was quantified experimentally and modeled numerically using static and dynamic finite element analyses. The numerical and experimental results agreed in identifying a correlation between ToF and IOP and CCT. However, some quantitative discrepancies between numerical and experimental results warrant the improvement of the model.

[1]University of Pittsburgh, Department of Civil & Environmental, 729 Benedum Hall, Pittsburgh, PA, 15261, USA, pir3@pitt.edu
[2]Department Electrical and Computer Engineering, 3700 O'Hara Street, 1132 Benedum Hall, University of Pittsburgh, Pittsburgh, PA, 15261, Madisonhodgson@pitt.edu
[3]PhD. Candidate, Department of Civil and Environmental Engineering, 3700 O'Hara Street, 724 Benedum Hall, University of Pittsburgh, Pittsburgh, PA, 15261, ALK438@pitt.edu
[4]Department Electrical and Computer Engineering, 3700 O'Hara Street, 1138 Benedum Hall, University of Pittsburgh, Pittsburgh, PA, 15261, dickerson@pitt.edu

INTRODUCTION

Glaucoma is an age-related disease characterized by optic neuropathy and progressive visual field loss. It is the second leading cause of blindness in the world [1], affecting nearly 80 million people worldwide, plus an estimated 40 million not formally diagnosed [2], [3]. When a patient's eye has an abnormal balance between the production and drainage of fluids, the intraocular pressure (IOP) can spike, damaging the optic nerve. To date, measuring IOP is the cornerstone of the diagnosis and management of glaucoma because elevated pressure is the only risk factor that can be modified. However, similar to circadian rhythm, eye pressure fluctuates throughout the day making a single IOP measurement taken during an office visit insufficient even when commercial tonometers such as the Goldmann applanation tonometer (GAT) [4], the Corvis ST [5], or the iCare Tonopen [6] are used. These three instruments must be administered by a healthcare professional and be proctored directly on the cornea resulting in an IOP measurement taken at a single point in time. To overcome such burden, some commercial systems for home tonometry have been developed [7-10].

In the study presented in this brief article, a conceptually novel tonometer was investigated with the long-term aim of developing an easy-to-use inexpensive device feasible for self-administration and tailored to the specific geometry of the patient's eyes. The core engineering principle is based on the propagation and detection of highly nonlinear solitary waves (HNSWs) along the chain. These waves are fundamentally different than those encountered in acoustics and ultrasound. Those waves are linear and are characterized by having a return force linearly dependent on the displacement. HNSWs are instead nonlinear and based on the Hertz's law [11].

The idea behind the novel tonometer stems from the work conducted by Rizzo and co-authors who pioneered the use of HNSWs for the nondestructive evaluation / structural health monitoring of civil engineering materials [12-15]. All these studies are based on the same principle. The last particle of the chain is in point contact with the material to be assessed. An incident solitary wave (ISW) is generated by lifting and releasing the topmost particle (the striker). The ISW travels to the point contact with the material to be evaluated; here, part of the energy reflects back giving rise to the primary reflected solitary wave (PSW). The remaining energy detaches the last particle from the chain to deform elastically the sample, triggering vibrations that may induce secondary reflected solitary waves (SSW) that trail the PSW. The amplitude of the reflected waves and the time delay, known as the time of flight (ToF), between the ISW and the reflected waves are influenced by the material's characteristics and are inferred noninvasively.

In this study, a tonometer based on this engineering principle was designed, assembled and tested to quantify the effects of the IOP and CCT on the wave characteristics. Five polydimethylsiloxane (PDMS) corneas, hereinafter referred to as cornea eyeball phantoms (CEP) were fabricated. Each sample was then pressurized from 12 mmHg to 26 mmHg in 1 mmHg increments and probed with the novel device. The same test protocol was also used to probe two ex-vivo lamb corneas obtained from a local abattoir. From the engineering standpoint, the novelty of this study lies on the new use of HNSWs for the noninvasive assessment of soft materials of different thicknesses and deformation. From a biomedical

perspective, this paper represents the first experimental proof that certain simple characteristics of HNSWs can be related to the internal pressure of PDMS and ex-vivo lamb corneas. The paper presented here is excerpted from a recent publications [16] and the authors are referred to that paper for more insights.

EXPERIMENTAL SETUP

The 1-D chain inside the tonometer has twenty-five 2.38 mm (0.094 in) diameter spheres. The striker and four particles are ferromagnetic whereas the remaining spheres are made of 304 stainless steel. Atop the chain, a commercial solenoid lifts and releases the striker from a height of 4.76 mm (0.188 in). Halfway through the chain, a 10 mm (0.394 in) long coil is wrapped around the four ferromagnetic particles. The coil sits between two permanent hollow cylindrical magnets, providing a constant magnetic field. The coil senses the solitary waves using the principle of inverse magnetostriction, which refers to the deformation of a ferromagnetic material when placed into a magnetic field. A coil-type sensor, similar to the one described, was used to detect guided ultrasonic waves in strands [17-18].

The PCB controls the solenoid, amplifies the detected signals with a gain of 8.2 V/V, samples at 875 kHz with an analog-to-digital converter, and stores the waveform with a microcontroller unit (MCU). The PCB also allows for the transmission of the signal via Bluetooth or serial communication to a laptop or tablet. In this study, the experimental waveforms were transmitted via USB cable, and a typical signal is shown in Fig. 2. The shape of the experimental waveforms is different than the gaussian-like shape of typical HNSW, for which the dynamic force is approximatively the fourth power of a cosine function. The main reason for such difference is related to the sensing mechanism. In most of the experimental HNSWS-based applications, load cells, piezo-wafers transducers, or laser vibrometers are used. The output of these devices is directly proportional to the compressive dynamic force generated by the propagation of the HNSWs. In contrast, the coil embedded in the proposed tonometer senses the change of the constant magnetic field induced by the permanent magnets. Specifically, when the solitary wave travels through the constant magnetic field, the wave increases the compression between two adjacent particles, yielding to a positive gradient of the magnetic flux, which in turn induces the positive voltage. When the pulse moves away, the dynamic compression disappears, a negative gradient of the magnetic flux is induced, and the output voltage has therefore a negative gradient.

Five molds were 3D printed using clear resin to make phantom corneas with thicknesses between 500 and 600 μm, the typical CCT range of healthy and glaucomatous eyes. The proxy corneas were made with PDMS obtained from Sylgard 184, a two-part (silicon base elastomer and curing agent) polymer.

The actual thicknesses of the samples were measured using Optical Coherence Tomography (OCT) while clamped in an artificial anterior chamber. The samples were 492 μm, 498 μm, 555 μm, 560 μm, and 634 μm thick.

In addition to the test specimens, three 18 mm × 18 mm (0.708 in x 0.708 in) coupons were also prepared and tested to infer the mechanical properties of the

PDMS. Two coupons were 3.44 mm (0.135 in) thick whereas the third coupon was 3.23 mm (0.127 in) thick. Compressive strains ranging from 0% to 10% of the sample's thickness were applied using an Instron 8874 machine on the same day of fabrication.

Figure 1 shows the stress-strain curve based on the engineering stress/strain values associated with the three coupons. The slope of the curve up to 3% deformation was considered to determine the Young's modulus. The average value of the three moduli equaled 453 kPa, which agrees with the clinical values found in glaucomatous patients.

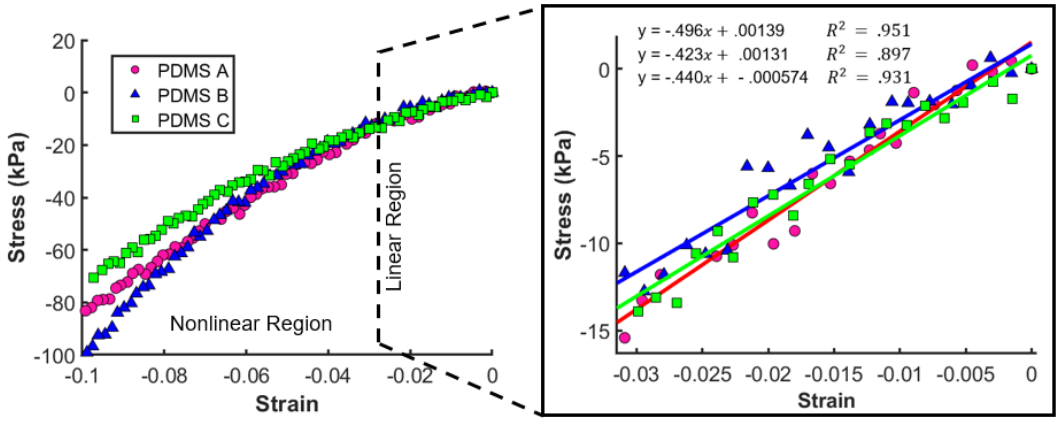

Figure 1 - Stress-strain diagram associated with the three PDMS coupons fabricated to characterize the Young modulus of PDMS. The linear regression within the 0-3% compressive strain was used to calculate the average Young's Modulus [16]

Two ex-vivo lamb eyes were obtained and tested in accordance with the tenets of the Declaration of Helsinki and the Association of Research in Vision and Ophthalmology's statement for the use of animals in ophthalmic and vision research. Once received, the globes had the episcleral tissues, fat, and muscles removed as seen in Fig. 2. The iris and lens were then carefully separated from the cornea and the sclera was trimmed to fit overtop the anterior chamber with the peak of the cornea sitting in the center. If any globes arrived damaged, or were damaged in the process of fixing to the anterior chamber, they were discarded.

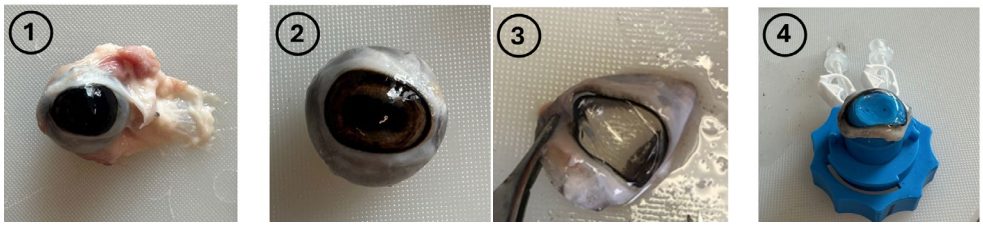

Figure 2 – Photos of one of the lamb corneas at different phase of the preparation [16].

Each specimen was pressurized from 12 mmHg to 26 mmHg in 1 mmHg increments. Pressure was induced by connecting one port of the anterior chamber to a water column while the other was connected to a pressure sensor which provided a feedback to a multi-directional water pump. One spout of the multi-directional water pump was connected via tubing to the water column while the other was fed into a water reservoir. The scheme of the whole setup is shown in Fig. 3.

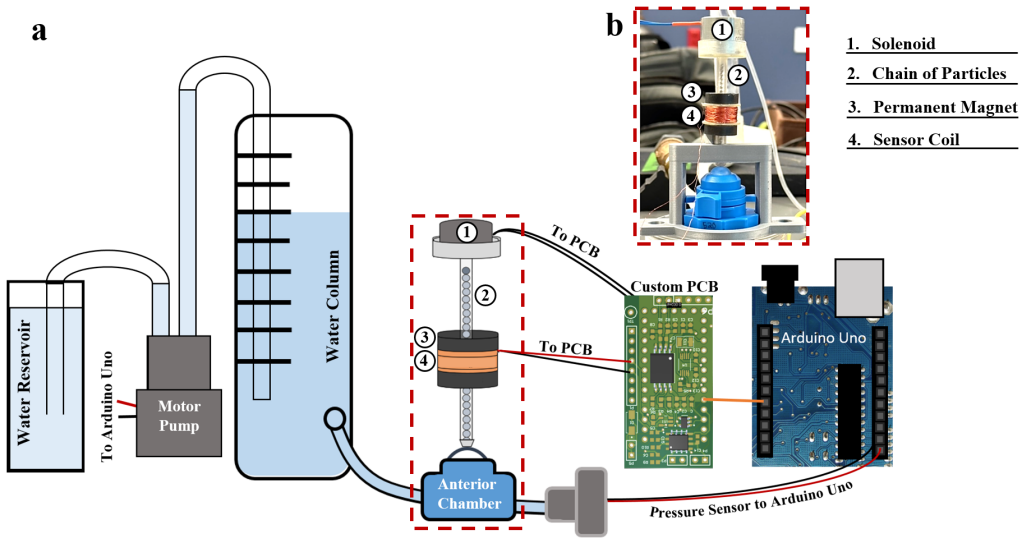

Figure 3 – (a) Scheme of the test setup.(b) Photo of the solitary wave transducer [16].

Besides controlling the tonometer, the PCB interfaced with a microcontroller, which drove the motor pump in a feedback loop. At any given pressure, the pressure was kept constant for the amount necessary to trigger and detect 15 striker impacts. After each impact, the PCB transmitted the waveform through serial communication. It is worth noting that the whole experiment for any given cornea was fully automatic.

During the experiment, the transducer was held atop the anterior chamber (Fig. 3b) with the bottom particle as the only point of contact with the specimen. As 15 measurements were taken for each pressure, 225 waveforms were collected at each ramp, and a total of 2,250 signals were collected.

The ex-vivo specimens were tested using the same protocol and only one loading ramp.

RESULTS

The time waveforms were post-processed in Matlab® software to calculate the ToF associated with the PSW and the SSW. As the experiment was fully automatic, a cross-check was executed to reject false positives, i.e. signals that were erroneously stored and transmitted but not associated with the physical phenomenon studied here. Only 7.3% of the 2,250 measurements from the PDMS corneas were rejected whereas for the ex-vivo corneas, 28.5% waveforms did not contain any reflected wave and 4.2% had large standard deviations.

The retained waveforms were used to quantify the effect of the IOP and CCT on the ToF of the reflected waves. Fig. 3 presents the ToF of the PSW against the IOP for all five artificial corneas. The results appear clustered in three groups based on thickness: 492 and 498 µm, 555 and 560 µm, and 643 µm. Each dot of Fig. 4 represents 30 measurements, 15 test runs for each of the two ramps. Because the stiffness is proportional to thickness, thinner specimens resulted in a higher travel time due to soft restitution of the ISW. On the other hand, when the stiffness of the bounding medium is high, the acoustic energy caused by the strong repulsion of the incident waves travels faster, and is carried mostly by the PSWs, leaving a small

portion of energy to the SSWs. Regardless of the thickness, the ToF is monotonically and inversely proportional to the pressure. As the pressure increases, the artificial cornea increases its resistance to deformation, thus reducing the rebound time. Fig. 4 validates the research hypotheses that the ToF of the solitary waves propagating along a chain of uniform particles is monotonically affected by both pressure and material thickness.

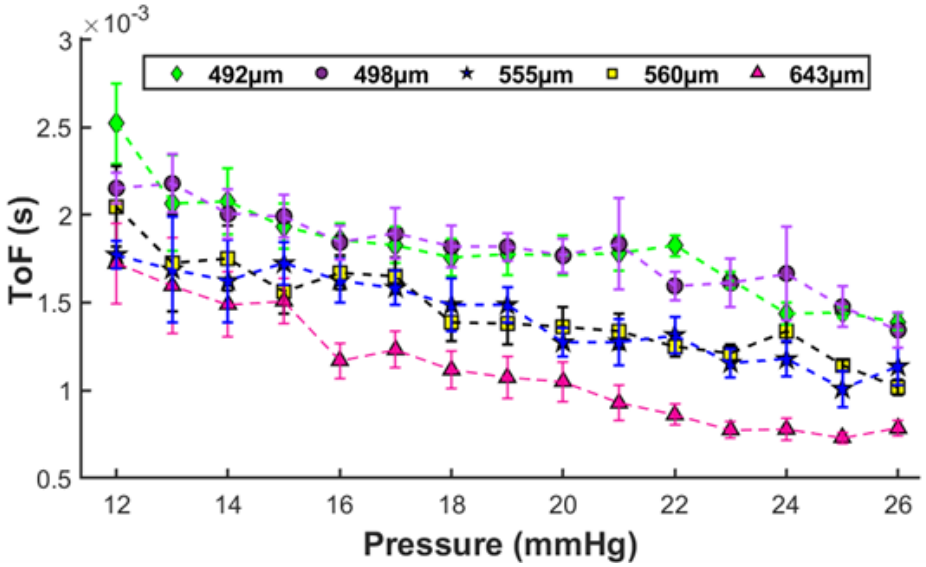

Figure 4 - ToF at each pressure for all 5 CEPs: 492 µm, 498 µm, 555 µm, 560 µm, and 643 µm.

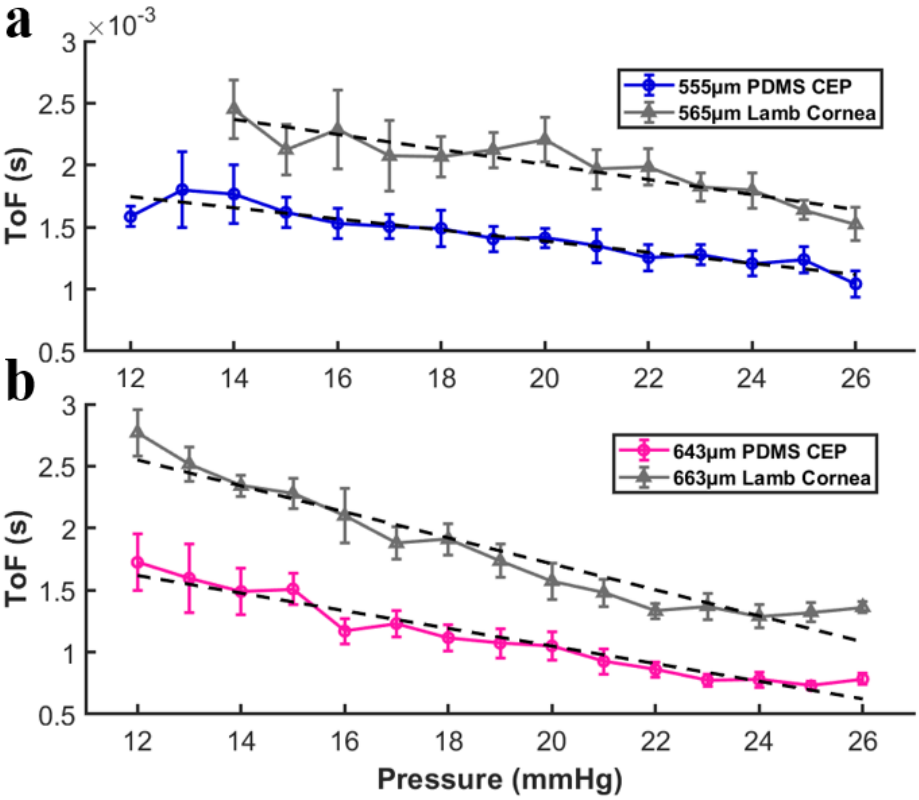

Figure 5 - PDMS CEPs compared to lamb corneas using the ToF of the PSW.

The results of the phantom corneas were compared with the results of the two lamb corneas. Pairs of samples with similar thicknesses were grouped and are shown in Fig. 5, where the ToF is plotted against the IOP. The vertical error bar represents the two standard deviations obtained from the signals retained at any given pressure. Fig. 5a compares the 555 μm thick PDMS sample to the 565 μm ex vivo cornea whereas Fig. 5b compares the 643 μm thick PDMS sample to the 663 μm ex vivo cornea. The trends and the ranges of each error bar are similar. However, the ToFs related to the lamb specimen are higher and the slopes are slightly different. This is attributed to the lower Young's modulus of lamb corneas compared to PDMS, despite the lamb corneas being slightly thicker. While this hypothesis could not be demonstrated experimentally using, for example, the Instron machine, the hypothesis corroborates the frequent absence of detectable reflections at 12 and 13 mmHg. The membrane was too soft to rebound the incoming solitary wave, thus no reflective waves form.

CONCLUSION

This article presented the first experimental evidence of a novel tonometer based on the generation, propagation, and detection of highly nonlinear solitary waves (HNSWs). The tonometer consists of a chain of spherical particles where a solenoid at one end of which triggers a HNSW. At the other end, the last particle is in contact with the cornea to be examined. The waves are measured using a coil wrapped around four ferromagnetic particles of the chain. The tonometer is completed with an electronic circuit that drives the solenoid, amplifies and samples the signals, and transmits the time waveforms through Bluetooth or serial communication.

Five artificial corneas made of PDMS and two ex-vivo lamb corneas were tested using a fully automatic test setup able to induce internal pressures between 12 mmHg and 26 mmHg at 1 mmHg step. The ToF of the waves reflected from the chain-cornea interface were found to be monotonically dependent on both the pressure and thickness as well as the modulus of the cornea. Specifically, the ToF decreases as pressure increases and decreases, at a given pressure, with the increase of the modulus and thickness. For example, the ToF of the 643 μm thick artificial cornea ranged between 1.8 ms and 0.6 ms compared to the ToF of the 492 μm thick cornea which ranged from approximately 2.5 ms to 1.4 ms.

Overall, the results of this study demonstrated the feasibility of the proposed biomedical device. The fact that the engineering principles exploited here are based on the dynamic interaction between waves and a cornea suggests that the proposed instrument may face the same challenges as tonometers based on dynamic impact. Owing to the scope of this article, the interested readers are referred to paper [16] for more insights about the setup and results of the study briefly presented here.

ACKNOWLEDGEMENTS

This work was supported by the U.S. National Science Foundation (NSF) Smart and Connected Health Program, Grant No. 2014389 with Dr. Wendy Nilsen as

program director. The authors would like to acknowledge Ms. Hannah Schilpp for the preparation and imaging of the lamb corneas in addition to the management of the eye measurement data. The authors also acknowledge the contribution of Mr. Jianzhe Luo for guidance during the PDMS compression test setup.

REFERENCES

[1] Glaucoma Research Foundation, "Glaucoma Facts And Stats - Glaucoma Research Foundation." Accessed: Jul. 02, 2024. [Online]. Available: https://glaucoma.org/articles/glaucoma-facts-and-stats

[2] R. N. Weinreb, "Glaucoma Worldwide: A Growing Concern | glaucoma.org." Accessed: Jan. 05, 2024. [Online]. Available: https://glaucoma.org/glaucoma-worldwide-a-growing-concern/

[3] S. Arora, C. J. Rudnisky, and K. F. Damji, "Improved Access and Cycle Time with an 'In-House' Patient-Centered Teleglaucoma Program Versus Traditional In-Person Assessment," *Telemed. E-Health*, vol. 20, no. 5, pp. 439–445, May 2014, doi: 10.1089/tmj.2013.0241.

[4] K. Mansouri, F. A. Medeiros, and R. N. Weinreb, "Effect of glaucoma medications on 24-hour intraocular pressure-related patterns using a contact lens sensor," *Clin. Experiment. Ophthalmol.*, vol. 43, no. 9, pp. 787–795, 2015, doi: 10.1111/ceo.12567.

[5] A. Boszczyk, H. Kasprzak, and D. Siedlecki, "Non-contact tonometry using Corvis ST: analysis of corneal vibrations and their relation with intraocular pressure," *J. Opt. Soc. Am. A Opt. Image Sci. Vis.*, vol. 36, no. 4, pp. B28–B34, Apr. 2019, doi: 10.1364/JOSAA.36.000B28.

[6] B. Cvenkel, M. A. Velkovska, and V. D. Jordanova, "Self-measurement with Icare HOME tonometer, patients' feasibility and acceptability," *Eur. J. Ophthalmol.*, vol. 30, no. 2, pp. 258–263, Mar. 2020, doi: 10.1177/1120672118823124.

[7] Y. Shigemoto *et al.*, "Repeated Measurements Are Necessary for Evaluating Accurate Diurnal Rhythm Using a Self-Intraocular Pressure Measurement Device," *J. Clin. Med.*, vol. 12, no. 7, p. 2460, Mar. 2023, doi: 10.3390/jcm12072460.

[8] J. J. Ogle, W. C. Soo Hoo, C. H. Chua, and L. W. L. Yip, "Accuracy and Reliability of Self-measured Intraocular Pressure in Glaucoma Patients Using the iCare HOME Tonometer," *J. Glaucoma*, vol. 30, no. 12, pp. 1027–1032, Dec. 2021, doi: 10.1097/IJG.0000000000001945.

[9] "Operation Manual," Tonometer Diaton. Accessed: Jul. 17, 2024. [Online]. Available: https://tonometerdiaton.com/guides-training/diaton-tonometer-operation-manual/

[10] I. K. Karunaratne *et al.*, "Wearable dual-element intraocular pressure contact lens sensor," *Sens. Actuators Phys.*, vol. 321, p. 112580, Apr. 2021, doi: 10.1016/j.sna.2021.112580.

[11] C. Daraio, V. F. Nesterenko, E. B. Herbold, and S. Jin, "Tunability of solitary wave properties in one-dimensional strongly nonlinear phononic crystals," *Phys. Rev. E*, vol. 73, no. 2, p. 026610, Feb. 2006, doi: 10.1103/PhysRevE.73.026610.

[12] X. Ni, P. Rizzo, J. Yang, D. Katri, and C. Daraio, "Monitoring the hydration of cement using highly nonlinear solitary waves," *NDT E Int.*, vol. 52, pp. 76–85, Nov. 2012, doi: 10.1016/j.ndteint.2012.05.003.

[13] L. Cai, P. Rizzo, and L. Al-Nazer, "On the coupling mechanism between nonlinear solitary waves and slender beams," *Int. J. Solids Struct.*, vol. 50, no. 25, pp. 4173–4183, Dec. 2013, doi: 10.1016/j.ijsolstr.2013.08.018.

[14] A. Bagheri, E. La Malfa Ribolla, P. Rizzo, L. Al-Nazer, and G. Giambanco, "On the Use of L-shaped Granular Chains for the Assessment of Thermal Stress in Slender Structures," *Exp. Mech.*, vol. 55, no. 3, pp. 543–558, Mar. 2015, doi: 10.1007/s11340-014-9964-1.

[15] X. Ni and P. Rizzo, “Highly Nonlinear Solitary Waves for the Inspection of Adhesive Joints,” *Exp. Mech.*, vol. 52, no. 9, pp. 1493–1501, Nov. 2012, doi: 10.1007/s11340-012-9595-3.
[16] Hodgson, M., Komaie, A., Dickerson, S., and Rizzo, P. (2025). “Measuring Intraocular Pressure using Solitary Waves,” Sensors and Actuators A: Physical, 389, 1 August 2025, 116521. https://doi.org/10.1016/j.sna.2025.116521.
[17] F. Lanza di Scalea, P. Rizzo, and F. Seible, “Stress Measurement and Defect Detection in Steel Strands by Guided Stress Waves,” *J. Mater. Civ. Eng.*, vol. 15, no. 3, pp. 219–227, Jun. 2003, doi: 10.1061/(ASCE)0899-1561(2003)15:3(219).
[18] P. Rizzo and F. L. di Scalea, “Feature Extraction for Defect Detection in Strands by Guided Ultrasonic Waves,” *Struct. Health Monit.*, vol. 5, no. 3, pp. 297–308, Sep. 2006, doi: 10.1177/1475921706067742.